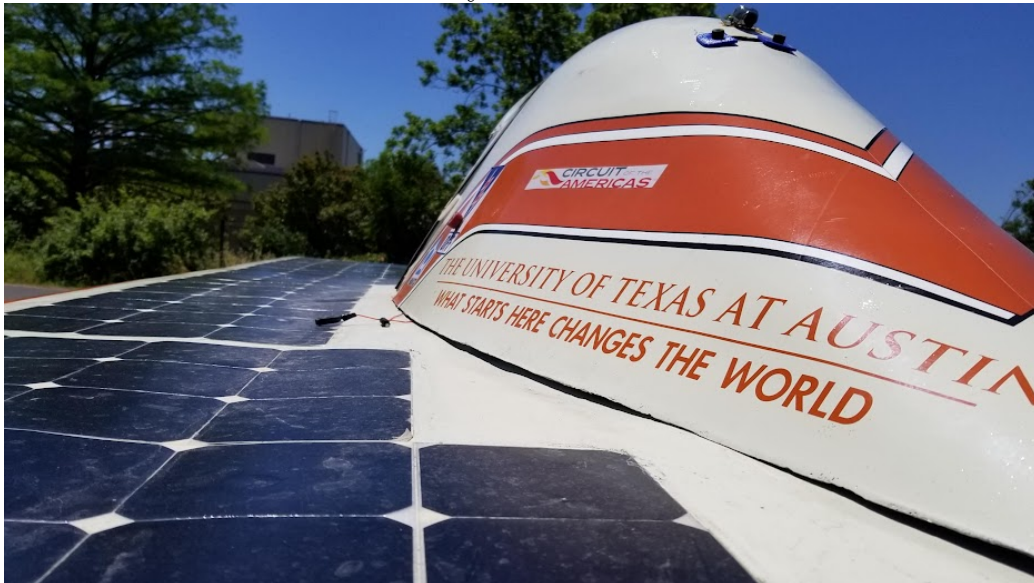


Evaluation and Improvement of Photovoltaic Power Systems

The University of Texas at Austin



Matthew Junkit Yu

16 December 2022

Contents

1	Introduction	4
2	Modeling Photovoltaics	7
2.1	Three Parameter Solar Cell Model	8
2.2	Five Parameter Solar Cell Model	16
2.3	Seven Parameter Solar Cell Model	17
2.4	Evaluating Solar Cell Models	18
3	Optimizing Photovoltaics	19
4	Optimizing Photovoltaic Systems	20
5	Conclusion	21
A	Acronyms and Abbreviations	22
A	Mathematical Nomenclature	23

List of Figures

2.1	Three Parameter, or Single Diode Model of a Solar Cell	8
2.2	Maxeon Gen III Cell Spectral Response	9
2.3	Solar Cell Temperature Dependence	11
2.4	Solar Cell Irradiance Dependence	12

List of Tables

Chapter 1

Introduction

In order to reach net zero emissions targets set by the United Nations (UN) at the 2015 Paris Agreement [9] before 2050, the International Energy Association (IEA) estimates that nearly 630 Gigawatts (GW) [7] of photovoltaic (PV) energy generation capacity need to be added annually by 2030. As of 2022, we observed that at least 175 GW were installed in 2021 [6] [5], a 22% year over year growth. With large policy and geopolitical tailwinds behind major economies like the United States and Europe, solar is expected to be one of the, if not the major driver of new energy generation within the next two decades.

However, in order to achieve this target generation capacity in a sustainable way, engineers and PV designers need to maximize the electrical efficiency of the overall power system, as opposed to just improving the solar cell efficiency. According to the U.S. Energy Information Administration (EIA) [11], the capacity factor of PVs as an energy source in the United States reached a monthly maximum of 33.4% in June of 2022; *capacity factor* is defined by the EIA as a measure of the generated output by the electric generator versus the maximum possible output. It is clear that system inefficiencies in PV generation provide large constraints, and optimistically, equally large opportunities, in allowing us to increase our pace towards reaching net zero carbon emissions by 2050.

This thesis takes a holistic evaluation of the PV power generation system in a unique use case that necessitates maximizing the capacity factor: solar powered vehicles. We evaluate the modeling, creation, and optimization of a solar powered vehicle for the University of Texas at Austin's Longhorn Racing Solar team, and attempt to identify and address inefficiencies and

bottlenecks whose improvements will help the larger PV industry as a whole.

In particular, this thesis will focus on three important and active areas of development within the PV field: solar array modeling and prediction, solar cell binning processes and heuristics, and maximum power point tracking algorithms. In each of these areas, we look at the state of the art techniques, propose novel ideas to improve our understanding of the system and its inefficiencies, and see if we can translate it lateral applications like rooftop solar or industrial PV. Note that in this thesis we refer to photovoltaics and solar without distinction.

In the first major section, **Modeling Photovoltaics**, this thesis discusses how can solar cells can be modeled at various abstraction layers, from idealized cells at standard conditions using the 3-parameter model to non-idealized cells that incorporate parasitic resistances using the 7-parameter model. These solar cell models are then evaluated against a dataset of several hundred solar cell current-voltage (I-V) curves generated from our custom testing setup to see how well the model fits real cells at different conditions. We build upon these models to form larger units of PVs, such as solar modules and solar arrays, which may consist of strings of cells in series with bypass diodes across them, among other configurations. Some important topics that are explored using these multi-cell models include PV mismatch and bypass activation. Insights from these topics lead to heuristics that are proposed in the next section, **Optimizing Photovoltaics**.

The second major section, **Optimizing Photovoltaics**, takes the aforementioned models and dataset created to propose a process to bin, match, and combine solar cells and modules, with the end goal of maximizing the performance of the solar array that will be attached to the solar vehicle. In this section, we propose design criteria, heuristics, and methodologies to generate designs for the solar vehicle that fit the unique constraints of the application, which center around the dynamism of the system as it moves in transit across the real world.

In the third and final major section, **Optimizing Photovoltaic Infrastructure**, this thesis investigates the operation of the PV system in the context of the solar vehicle. We observe the energy conversion process from incident light on the solar array to electricity captured by the battery protection system (BPS) and present a PV system simulator and a suite of maximum power point tracking (MPPT) algorithms to minimize energy losses from the aforementioned conversion process. We demonstrate custom hardware developed by the Longhorn Racing Solar team and evaluate in real

The second area of development may be more generalized then this.

world settings a select set of MPPT algorithms. We compare these results with existing research and our digital twin model of the solar vehicle, and finally discuss conclusions from the three sections that can be translatable to the wider PV industry.

Along with these three major sections, we also provide a large set of appendices corresponding to the development of the main body of work in this thesis. Among them include manufacturing procedures for testing, assembling, and laminating solar cells into solar modules, schematics and accompanying documentation for hardware that was used for characterizing and validating parts of the thesis, software diagrams with relevant open source software repositories developed by our team, and extra insights into the design of the Longhorn Racing Solar’s photovoltaic array that are not directly applicable to the major sections, such as thermal models performed of the vehicle topshell that influenced our simulation models, among others.

Chapter 2

Modeling Photovoltaics

Insert intro paragraph on the focus of this chapter, as well as the a short discussion of the following sections.

2.1 Three Parameter Solar Cell Model

The most basic model of a solar cell is the three parameter model, or single diode model. It consists of a constant current source that produces photocurrent (I_{PV}), and a diode that consumes part of I_{PV} in the form of dark current, or diode current (I_D). The remaining load current (I) is left to be sunk into the load resistance (R_L). We consider this model ideal, since it does not incorporate cell losses in the form of series resistance (R_S) and shunt resistance (R_{SH}). It is assumed that the series resistance is zero or short circuit and the shunt resistance is infinite or open circuit. This is addressed in the five parameter and seven parameter models.

The load current I in Figure 2.1 can be represented as a function of the photocurrent I_{PV} and the dark current I_D , shown in Equation 2.1.

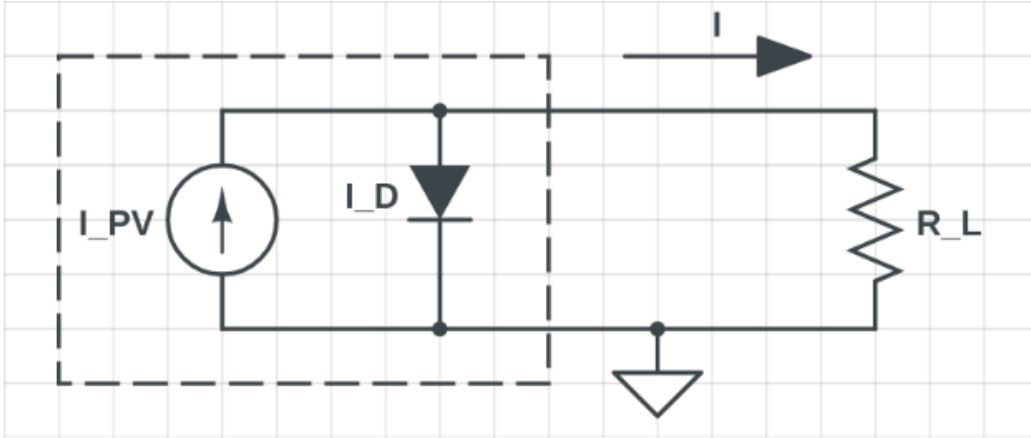


Figure 2.1: Three Parameter, or Single Diode Model of a Solar Cell

$$I = I_{PV} - I_D \quad A \quad (2.1)$$

Photocurrent and Short Circuit Current

On a fundamental level, we can define the photocurrent I_{PV} as a function of the photons incident upon the surface of the solar cell and the spectral response of the solar cell. This is demonstrated in Equation 2.2. A bulleted explanation of this equation oriented for the layman is as follows:

$$I_{PV} = qA \int b_s(E)QE(E)dE \quad A \quad (2.2)$$

- Incident light hits the solar cell over a given spectrum of energy levels (denoted either in eV or in nm) (see Figure 2.2).
- Incident light at each discrete energy level has an spectral photon flux density ($b_s(E)$), otherwise known as intensity.
- The solar cell has a given quantum efficiency ($QE(E)$) at each energy level, which is the probability that an incident photon of energy (E) delivers one electron to the external circuit.
- Integrating the product of the photon flux density $b_s(E)$ and quantum efficiency $QE(E)$ (then multiplied by the electric charge constant (q) and the cell area (A)) provides the photocurrent I_{PV} .

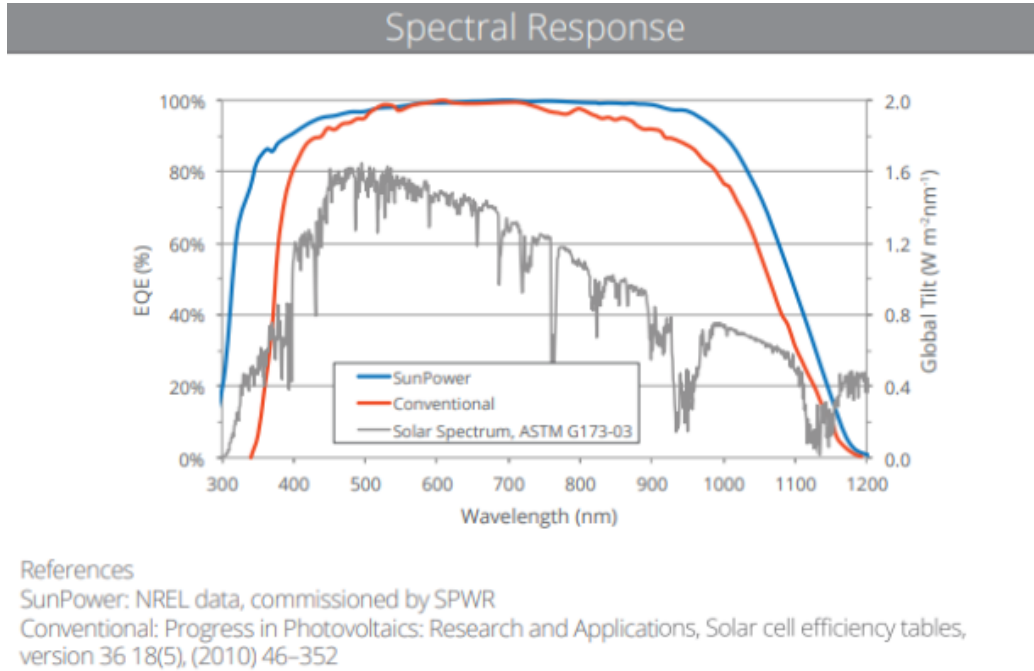


Figure 2.2: Maxeon Gen III Cell Spectral Response

Solar cell manufacturers may provide a spectral response chart showing the quantum efficiency over the useful solar spectrum (as seen in Figure 2.2), but will generally just provide the short circuit current (I_{SC}) at standard test conditions (STC) (1000 Wm^{-2} , $AM \ 1.5G$, $25 \text{ }^\circ\text{C}$).

As it turns out, the photocurrent I_{PV} can generally be approximated as the short circuit current I_{SC} .

$$I_{PV} = I_{SC} \text{ A} \quad (2.3)$$

We'll discuss in a further section that Cubas et al. [8] defines the photocurrent as a ratio of the series and shunt resistance in addition to the short circuit current. However, in most cases the empirical value of I_{SC} does not differ from Equation 2.3.

Dark Current

The dark current I_D comprises of the interesting and critical parameters of the three parameter model shown in Equation 2.4; it contains the dark saturation current (I_0) and an exponential. The exponential is a function of cell temperature (T_C) and load voltage (V) applied across the cell. The term thermal voltage (V_T) which encapsulates the T_C dependence describes the voltage across the P-N junction of the diode in the model: at STC this is typically 26 mV . It is defined by Equation 2.5.

$$I_D = I_0 \left[\exp\left(\frac{V}{V_T}\right) - 1 \right] \text{ A} \quad (2.4)$$

$$V_T = \frac{k_B T_C}{q} \text{ V} \quad (2.5)$$

Dark Saturation Current

The dark saturation current I_0 has two potential derivations. Generally, the three parameter model, (see Baig et al. [1], MacAlpine et Brandemuehl [4], Rusirawan et Farkas [10], and others) define I_0 as in Figure 2.6; where the diode current is a function of the cell temperature and the energy bandgap in relation to a several reference parameters at STC. These terms cancel each other out in the exponential, so the eventual subtraction is unitless.

$$I_0 = I_{0,ref} \left(\frac{T_C}{T_{C,ref}} \right)^3 \exp \left(\frac{E_{G,ref}}{k_B T_{C,ref}} - \frac{E_G}{k_B T_C} \right) A \quad (2.6)$$

On the other hand, we can derive the I_0 numerically, given I_{SC} and open circuit voltage (V_{OC}), by setting the cell at open circuit: at open circuit, there is no load therefore the cell is at V_{OC} . This is shown by Figure 2.7.

$$I_0 = I_{SC} \left[\exp \left(\frac{V_{OC}}{V_T} \right) - 1 \right]^{-1} A \quad (2.7)$$

These two models of the reverse saturation current will be explored further in this major section.

Short Circuit Current

Finally, for the three parameter model, we derive the dependence of I_{SC} and V_{OC} on irradiance and temperature before establishing the final derivation of Equation 2.1.

It is known that for the short circuit current, there is a large positive correlation with irradiance and a small positive correlation with temperature, shown in Figures 2.3 and 2.4.

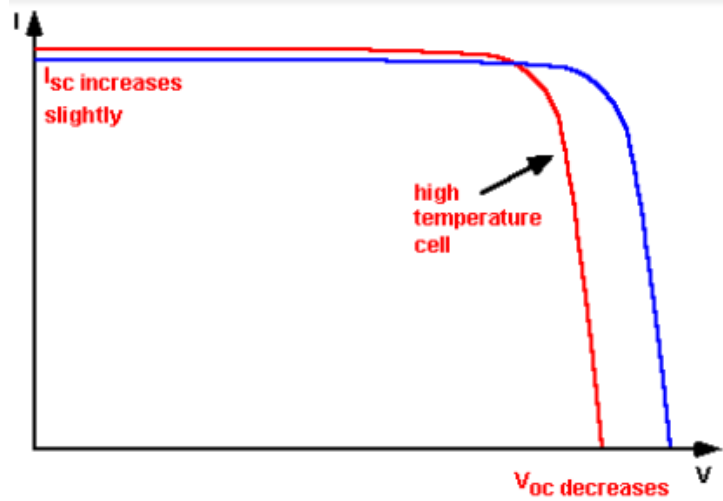


Figure 2.3: Solar Cell Temperature Dependence

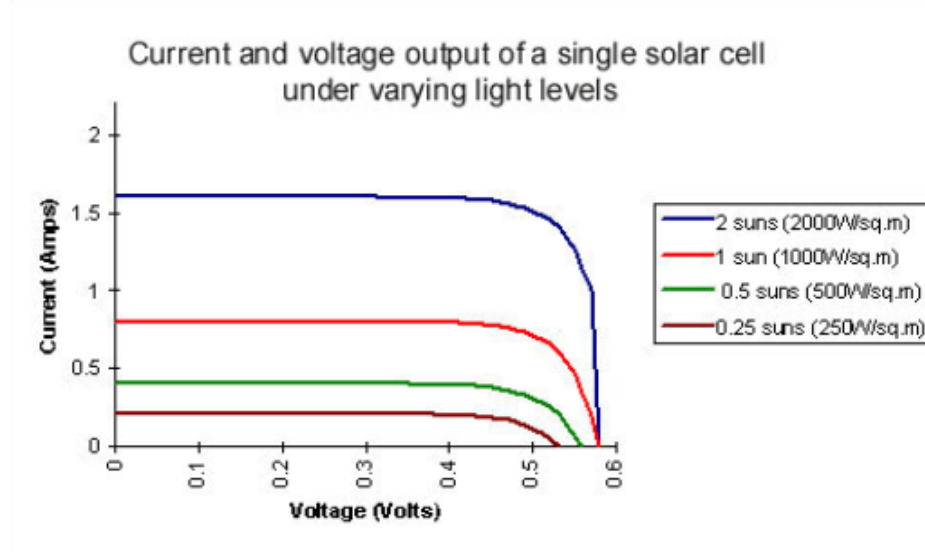


Figure 2.4: Solar Cell Irradiance Dependence

The dependence of irradiance on short circuit current can be modeled as linearly proportional to the light incident upon the solar cell over the reference irradiance. This makes intuitive sense: given half the available light (assuming the distribution of light across the spectrum is consistent), the solar cell will only be able to capture half the maximum available power. Chegaar et al. [2] proposes this relationship as Equation 2.8, where the short circuit current is a function of short circuit constant (K_E) and irradiance (G) in Wm^{-2} .

$$I_{SC}(G) = K_E G \text{ A} \quad (2.8)$$

Equation 2.8 can be easily reworked where the constant K_E is now based on a reference short circuit current and irradiance, preferably at STC. This forms Equation 2.9, which is the same form used by Baig et al. [1].

$$I_{SC}(G) = I_{SC,ref} \frac{G}{G_{ref}} \text{ A} \quad (2.9)$$

Hishikawa et al. [3] proposes modeling the dependence of temperature on short circuit current density using a thermal coefficient, α . α is empirically determined given the material composition and structure of the solar cell; for crystalline silicon solar cells, this is approximately 0.05%/K, or 0.0005.

Equation 2.10 shows how given α the change in temperature affects short circuit current density and vice versa. Rearranging the equation leads to the derivation Equation 2.11.

$$\alpha = \frac{1}{I_{SC,ref}} \frac{\Delta I_{SC}}{\Delta T_C} = \frac{1}{I_{SC,ref}} \frac{I_{SC,ref} - I_{SC}}{T_{C,ref} - T_C} \quad (2.10)$$

$$I_{SC}(T_C) = I_{SC,ref}[1 - \alpha(T_{C,ref} - T_C)] A \quad (2.11)$$

Interestingly, Rusirawan et Farkas [10] and MacAlpine et Brandemuehl [4] perform two different variants: Rusirawan et Farkas models the temperature dependence as a ..., shown in Equation 2.12, and MacAlpine et Brandemuehl models the temperature dependence as a ..., shown in Equation 2.14.

$$I_{SC}(T_C) = I_{SC,ref} + \mu(T_{C,ref} - T_C) A, \text{ where} \quad (2.12)$$

$$\mu = \frac{I_{SC} - I_{SC,ref}}{T_C - T_{C,ref}} = -\alpha \quad (2.13)$$

$$I_{SC}(T_C) = I_{SC,ref}[I_{SC,ref} + \alpha(T_{C,ref} - T_C)] A \quad (2.14)$$

Combining Equations 2.9 and 2.11 give us Equation 2.15.

$$I_{SC}(G, T_C) = I_{SC,ref} \frac{G}{G_{ref}} [1 - \alpha(T_{C,ref} - T_C)] A \quad (2.15)$$

These three models of the short circuit current will also be explored further in this major section.

Open Circuit Voltage

Likewise, the open circuit voltage is also a function of temperature and irradiance. It is known that the open circuit voltage has a medium positive correlation with irradiance and a medium negative correlation with temperature, shown back in Figures 2.3 and 2.4.

Returning to Equation 2.7, in which we defined the dark saturation current I_0 as a function of the open circuit voltage V_{OC} , we can invert the equation to retrieve the V_{OC} parameter, shown in Equation 2.16.

$$V_{OC} = V_T \ln\left(\frac{I_{SC}}{I_0} + 1\right) V \quad (2.16)$$

Describe the differentiation between these three variants of I_{SC}

There are three points in this equation that can now be determined. We know from Equation 2.5 that the thermal voltage is dependent on the cell temperature T_C . We can also plug in one of the proposed models for I_{SC} . However, we cannot reuse Equation 2.7 because Equation 2.16 was derived from it! Chegaar et al. [2] simplifies the logarithmic term to form Equation 2.17.

$$V_{OC}(G, T_C) = V_{OC,ref} + V_T(T_C) \ln\left(\frac{G}{G_{ref}} + 1\right) V \quad (2.17)$$

This term fits well with the paper's experimental data, but is not immediately clear how it models the original term. It also does not properly model temperature change. Equation 2.18 is a modified form that implements temperature dependence while retaining irradiance dependence.

$$V_{OC}(G, T_C) = V_{OC,ref}[1 - \beta(T_{C,ref} - T_C)] + \frac{k_B(T_{C,ref} + T_C/\gamma)}{q} \ln\left(\frac{G}{G_{ref}}\right) V \quad (2.18)$$

$$\beta = \frac{1}{V_{OC,ref}} \frac{\Delta V_{OC}}{\Delta T_C} = \frac{1}{V_{OC,ref}} \frac{V_{OC,ref} - V_{OC}}{T_{C,ref} - T_C} \quad (2.19)$$

Equation 2.18 implements two changes: a linear constant β that represents the open circuit voltage temperature coefficient and a modifier T_C/γ . β is likewise empirically determined given the material composition and structure of the solar cell; for silicon it known to be -0.3%/K, or 0.003.

This fits expected data from other papers, but need to test on our setup.

The modifier is an experimentally determined curve fitting term, and appropriately models the exponential decrease of V_{OC} at low light conditions. It has an operable range of values between $[1, 100]$, where smaller values means a wider range of V_{OC} movement at low light conditions.

Model Summary

I don't agree with I_{PV} , I_D , and ideality factor (n) being the "parameters". It makes more sense for G , T_C , α , β , and γ to be the parameters, since they are actually empirically measured/changed.

To conclude this major section, let's bring in all the pieces developed by this model. Firstly, we know that the load current for the single diode solar cell model is dependent on two primary components: photocurrent source and a dark current sink. These two components are dependent on a set of intrinsic and extrinsic factors, namely build quality and uniformity, irradiance, temperature, and load.

The three parameters in this model are the two components aforementioned plus an n . This factor is between 1 and 2, and is a proxy for cell recombination.

The final model function is presented in Equation 2.20.

$$\begin{aligned}
 I(V, G, T_C) = & I_{SC,ref} \frac{G}{G_{ref}} [1 - \alpha(T_{C,ref} - T_C)] - \\
 & I_{SC,ref} \frac{G}{G_{ref}} [1 - \alpha(T_{C,ref} - T_C)] \\
 & \left[\exp\left(\frac{V_{OC,ref}[1 - \beta(T_{C,ref} - T_C)] + \frac{nk_B(T_{C,ref} + T_C/\gamma)}{q} \ln(\frac{G}{G_{ref}})}{\frac{nk_B T_C}{q}}\right) - 1 \right]^{-1} \\
 & \left[\exp\left(\frac{V}{\frac{nk_B T_C}{q}}\right) - 1 \right] A
 \end{aligned} \tag{2.20}$$

See <https://www.desmos.com/calculator/yp0rhmabkz> to play around with model. Add as figure later on compared to experimental data.


2.2 Five Parameter Solar Cell Model

2.3 Seven Parameter Solar Cell Model

2.4 Evaluating Solar Cell Models

Solar Cell Dataset

Methods to Fit Cells



Refer
to Ap-
pendix
for test-
ing setup

Chapter 3

Optimizing Photovoltaics

Chapter 4

Optimizing Photovoltaic Systems

Insert
sankey
diagram
from in-
cident
light to
battery
input

Chapter 5

Conclusion

Appendix A

Acronyms and Abbreviations

BPS	battery protection system
EIA	U.S. Energy Information Administration
GW	Gigawatts
IEA	International Energy Association
I-V	current-voltage
PV	photovoltaic
P-V	power-voltage
STC	standard test conditions
UN	United Nations

Appendix A

Mathematical Nomenclature

A area

$b_S(E)$ spectral photon flux density

E energy

G irradiance

I load current

I_D dark current, or diode current

I_{PV} photocurrent

I_{SC} short circuit current

I_0 dark saturation current

K_B Boltzmann constant

K_E short circuit constant

n ideality factor

$QE(E)$ quantum efficiency

q electric charge constant

R_L load resistance

R_S series resistance

R_{SH} shunt resistance

T_C cell temperature

V load voltage

V_T thermal voltage

V_{OC} open circuit voltage

Bibliography

- [1] Mirza Qutab Baig, Hassan Abbas Khan, and Syed Muhammad Ahsan. “Evaluation of solar module equivalent models under real operating conditions—A review”. In: *Journal of Renewable and Sustainable Energy* 12.1 (2020), p. 012701. DOI: 10.1063/1.5099557. eprint: <https://doi.org/10.1063/1.5099557>. URL: <https://doi.org/10.1063/1.5099557>.
- [2] M. Chegaar et al. “Effect of Illumination Intensity on Solar Cells Parameters”. In: *Energy Procedia* 36 (2013). TerraGreen 13 International Conference 2013 - Advancements in Renewable Energy and Clean Environment, pp. 722–729. ISSN: 1876-6102. DOI: <https://doi.org/10.1016/j.egypro.2013.07.084>. URL: <https://www.sciencedirect.com/science/article/pii/S1876610213011703>.
- [3] Yoshihiro Hishikawa et al. “Temperature dependence of the short circuit current and spectral responsivity of various kinds of crystalline silicon photovoltaic devices”. In: *Japanese Journal of Applied Physics* 57.8S3 (July 2018), 08RG17. DOI: 10.7567/JJAP.57.08RG17. URL: <https://dx.doi.org/10.7567/JJAP.57.08RG17>.
- [4] Sara M. MacAlpine and Michael J. Brandemuehl. “Photovoltaic module model accuracy at varying light levels and its effect on predicted annual energy output”. In: *2011 37th IEEE Photovoltaic Specialists Conference*. 2011, pp. 002894–002899. DOI: 10.1109/PVSC.2011.6186551.
- [5] Gaetan Masson et al. *Snapshot of Global PV Markets 2022 Task 1 Strategic PV Analysis and Outreach PVPS*. Apr. 2022. ISBN: 978-3-907281-31-4.
- [6] Gaetan Masson et al. *Trends in Photovoltaic Applications 2022*. Oct. 2022. ISBN: 978-3-907281-35-2.

- [7] *Net Zero by 2050*. Paris: IEA Photovoltaic Power Systems Programme, 2021.
- [8] Santiago Pindado, Javier Cubas, and Carlos Manuel. “Explicit Expressions for Solar Panel Equivalent Circuit Parameters Based on Analytical Formulation and the Lambert W-Function”. In: *Energies* 7 (June 2014), pp. 4098–4115. DOI: 10.3390/en7074098.
- [9] United Nations Environment Programme. *Paris Agreement*. 12/12/2015. URL: <https://wedocs.unep.org/20.500.11822/20830>.
- [10] Dani Rusirawan and István Farkas. “Identification of Model Parameters of the Photovoltaic Solar Cells”. In: *Energy Procedia* 57 (2014). 2013 ISES Solar World Congress, pp. 39–46. ISSN: 1876-6102. DOI: <https://doi.org/10.1016/j.egypro.2014.10.006>. URL: <https://www.sciencedirect.com/science/article/pii/S1876610214013733>.
- [11] Brady Tyra et al. *Electric Power Monthly*. U.S. Energy Information Administration, Oct. 2022. URL: <https://www.eia.gov/electricity/monthly/archive/october2022.pdf>.

TODOS

■ The second area of development may be more generalized then this.	5
■ Insert intro paragraph on the focus of this chapter, as well as the a short discussion of the following sections.	7
■ Describe the differentiation between these three variants of I_{SC} . . .	13
■ This fits expected data from other papers, but need to test on our setup.	14
■ I don't agree with I_{PV} , I_D , and n being the "parameters". It makes more sense for G , T_C , α , β , and γ to be the parameters, since they are actually empirically measured/changed.	14
■ See https://www.desmos.com/calculator/yp0rhmabkz to play around with model. Add as figure later on compared to experimental data.	15
■ Refer to Appendix for testing setup	18
■ Insert sankey diagram from incident light to battery input	20